

118893

Small molecule inhibitors confirm ubiquitin-dependent removal of TOP2-DNA covalent complexes¹

Rebecca L. Swan, Luke L.K. Poh, Ian G. Cowell* and Caroline A. Austin*

Newcastle University Biosciences Institute, Newcastle University, Newcastle upon Tyne. NE2 4HH. U.K. (R.L.S., L.L.K.P., I.G.C. & C.A.A.)

¹This study was supported by Bloodwise [Research Specialist Program Grant No. 12031 and Gordon Piller Studentship 13063].

118893

Running title: Ubiquitination is required for TOP2-DNA complex removal

Corresponding authors

To whom correspondence should be addressed:

Dr Ian G. Cowell and Professor Caroline A. Austin

Newcastle University Biosciences Institute, Newcastle University, Newcastle upon Tyne. NE2 4HH. United Kingdom

Tel: +44 (0)191 208 7677

Fax: +44 (0)191 208 7424

Email: ian.cowell@ncl.ac.uk, caroline.austin@ncl.ac.uk

Manuscript information

36 text pages including references and Figure legends

6 figures

0 tables

54 number of references

193 words in abstract

932 words in Introduction

1101 words in Discussion

Non-standard abbreviations

DMSO, Dimethyl sulfoxide; DSB, DNA double-strand break; UAE, ubiquitin activating enzyme, SAE, SUMO activating enzyme; H2AX, histone H2A.X; γH2AX, S-139 phospho-histone H2A.X; TOP2A, DNA Topoisomerase IIα; TOP2B, DNA topoisomerase IIβ; TOP2, DNA topoisomerase 2.

Keywords: DNA topoisomerase II / etoposide / proteasome / ubiquitin

118893

Abstract

DNA Topoisomerase II (TOP2) is required for the unwinding and decatenation of DNA through the induction of an enzyme-linked double strand break (DSB) in one DNA molecule, and passage of another intact DNA duplex through the break. Anticancer drugs targeting TOP2 (TOP2 poisons) prevent religation of the DSB and stabilise a normally transient intermediate of the TOP2 reaction mechanism called the TOP2-DNA covalent complex. Subsequently, TOP2 remains covalently bound to each end of the enzyme bridged DSB, which cannot be repaired until TOP2 is removed from the DNA. One removal mechanism involves the proteasomal degradation of the TOP2 protein, leading to the liberation of a protein-free DSB. Proteasomal degradation is often regulated by protein ubiquitination, and here we show that inhibition of ubiquitin activating enzymes reduces the processing of TOP2A- and TOP2B- DNA complexes. Depletion or inhibition of ubiquitin activating enzymes indicated that ubiquitination was required for the liberation of etoposide-induced protein-free DSBs and is therefore an important layer of regulation in the repair of TOP2 poison-induced DNA damage. TOP2-DNA complexes stabilised by etoposide were shown to be conjugated to ubiquitin and this was reduced by inhibition or depletion of ubiquitin activating enzymes.

Significance statement

There is currently great clinical interest in the ubiquitin-proteasome system and ongoing development of specific inhibitors. The results in this paper show that the therapeutic cytotoxicity of TOP2 poisons can be enhanced through combination therapy with UAE inhibitors, or by specific inhibition of the BMI/RING1A ubiquitin ligase which would lead to increased cellular accumulation or persistence of TOP2-DNA complexes.

118893

Introduction

DNA Topoisomerase II (TOP2) mediates important changes in DNA topology that are essential for processes such as chromosome condensation, chromosome segregation, replication and transcription (Nitiss, 2009a; Pommier *et al.*, 2016). These enzymes catalyse a “strand passage” mechanism whereby one double stranded DNA molecule is passed through a double-stranded break in another. TOP2 forms an intermediate enzyme-bridged DNA gate termed the TOP2-DNA covalent complex (or cleavage complex), where each monomer of the dimeric TOP2 molecule is covalently bound to one end of the DSB through a 5'-phosphotyrosyl bond. Following strand passage, the break is re-ligated and TOP2 dissociates from DNA. As the DSB is covalently coupled to and buried within the TOP2 enzyme, DNA cleavage does not initiate the DNA damage response that is generally observed following the appearance of DSBs (Mårtensson *et al.*, 2003).

The ability of TOP2 to induce DSBs is exploited in cancer therapy through the use of TOP2 poisons which inhibit the re-ligation of the enzyme-induced DSB and lead to the persistence of DSBs concealed by TOP2-DNA covalent complexes (Nitiss, 2009b). DNA repair requires the liberation of the DSB, which occurs upon the removal of TOP2 protein from the TOP2-DNA complex (Mårtensson *et al.*, 2003). TOP2-DNA covalent complexes can be removed through proteasomal degradation of TOP2 (Mao *et al.*, 2001; Zhang *et al.*, 2006; Fan *et al.*, 2008; Lee *et al.*, 2016), leaving behind a residual phosphotyrosyl peptide adduct which can then be removed by the 5'-phosphodiesterase, TDP2 (Cortes Ledesma *et al.*, 2009; Zeng *et al.*, 2011; Schellenberg *et al.*, 2012; Gao *et al.*, 2014). Alternatively, stabilised TOP2-DNA complexes can be processed in a nuclease-dependent pathway involving Mre11 (of

118893

the MRN complex), which may be stimulated by CtIP (Neale *et al.*, 2005; Hartsuiker *et al.*, 2009; Hamilton and Maizels, 2010; Nakamura *et al.*, 2010; Lee *et al.*, 2012; Aparicio *et al.*, 2016; Hoa *et al.*, 2016; Wang *et al.*, 2017). Other proteasome-independent mechanisms of TOP2-DNA complex processing have also been described, including the direct removal of TOP2 by TDP2 in cooperation with the ZATT SUMO ligase (Schellenberg *et al.*, 2016, 2017). Inactivation of TDP2 does not significantly affect the processing of TOP2-DNA complexes to DSBs in proteasome-inhibited cells, suggesting the majority of TOP2-DNA complexes are removed by pathways other than the TDP2/ZATT-dependent pathway (Lee *et al.*, 2018).

There are two TOP2 isoforms in human cells (TOP2A and TOP2B), and both form stabilised TOP2-DNA complexes in the presence of TOP2 poisons (Willmore *et al.*, 1998). Earlier publications suggested that TOP2B complexes are preferentially degraded (Mao *et al.*, 2001; Isik *et al.*, 2003; Azarova *et al.*, 2007). However, later papers have demonstrated that TOP2A is also degraded by the proteasome in response to TOP2 poisons including etoposide, teniposide, and mitoxantrone (Zhang *et al.*, 2006; Fan *et al.*, 2008; Alchanati *et al.*, 2009; Lee *et al.*, 2016). This was demonstrated both by western blot (Fan *et al.*, 2008; Alchanati *et al.*, 2009), and through direct measurement of TOP2-DNA complexes using the ICE assay (Fan *et al.*, 2008) and TARDIS assay (Sunter *et al.*, 2010; Lee *et al.*, 2016). The half-life of TOP2B-DNA complexes is shorter than that of TOP2A (Willmore *et al.*, 1998; Errington *et al.*, 2004; Lee *et al.*, 2016), which may account for the perceived “preferential degradation” of TOP2B. The processing of TOP2-DNA complexes can also be investigated through the measurement of TOP2 poison-induced DSBs. As alluded to above, DSBs buried within TOP2-DNA complexes do not themselves elicit a DNA damage response in the form of histone H2AX phosphorylation unless the complexes

118893

are processed to protein-free DSBs. Indeed, TOP2 poison-induced γ H2AX levels (and other markers of DNA damage) are reduced by co-treatment of cells with a proteasome inhibitor (Zhang *et al.*, 2006; Fan *et al.*, 2008; Tammaro *et al.*, 2013), consistent with a role for the proteasome in the liberation of protein-free DSBs from TOP2-DNA complexes.

Proteasomal degradation often (but not always) requires the ubiquitination of the target protein, which is catalysed by a ubiquitin activating enzyme, (UAE). Two studies investigating the requirement for UAE in the processing of TOP2-DNA complexes have yielded conflicting results. While both studies employed the same murine cell line ts85 containing a temperature sensitive UAE, growth at the non-permissive temperature curtailed TOP2 poison-induced depletion of TOP2B in the first study, but did not affect TOP2 poison-induced depletion of TOP2B in the second study (Mao *et al.*, 2001; Ban *et al.*, 2013). Thus, both ubiquitin-dependent and ubiquitin-independent mechanisms for TOP2B protein degradation have been hypothesised. In this study we seek to clarify the requirement of ubiquitination for the processing of TOP2-DNA covalent complexes. This was investigated by inactivation of UAE using a combination of siRNA knockdown and small molecule inhibitor approaches. MLN7243 is a potent E1 inhibitor which forms an MLN7243-ubiquitin adduct, leading to inhibition of both UAE enzymes in human cells (UAE1 and UBA6) (Misra *et al.*, 2017; Hyer *et al.*, 2018).

Previous studies have mainly used western blotting techniques to study the degradation of TOP2 upon etoposide or teniposide treatment. Here we use the TARDIS (Trapped in Agarose DNA Immunostaining) assay to investigate the effect of UAE inhibition. TARDIS is an immunofluorescence-based technique that visualises covalently bound TOP2-DNA complex levels in individual cells in a quantifiable

118893

manner. This contrasts with other techniques such as the ICE assay, which examines pooled cell populations. The processing of TOP2-DNA complexes was also investigated using the γ H2AX assay to measure the appearance of TOP2-free DSBs. We show that UAE activity is required for the efficient removal of both TOP2A- and TOP2B- complexes from DNA and the subsequent appearance of TOP2-free DSBs, indicating a ubiquitin-dependent processing pathway.

118893

Materials and methods

Cell culture and reagents

K562 cells and the human pre-B cell line Nalm-6 and the *TOP2B*^{-/-} derivatives of Nalm-6 were grown in RPMI medium containing 10% foetal bovine serum (FBS) and 5% penicillin-streptomycin (%v/v), and incubated at 37°C, 5% CO₂. Etoposide and MG132 were purchased from Sigma-Aldrich (Dorset, UK). MLN7243 (TAK-243, Sulfamic acid, ((1R,2R,3S,4R)-2,3-dihydroxy-4-((2-(3-((trifluoromethyl)thio)phenyl)pyrazolo(1,5-a)pyrimidin-7-yl)amino)cyclopentyl)methyl ester) (Hyer *et al.*, 2018) was purchased from Active Biochem (Hong Kong). PRT4165 (Ismail *et al.*, 2013) (2-Pyridin-3-ylmethylene-indan-1,3-dione) was purchased from Merck Millipore. UAE1 and UBA6 siRNA was purchased from ThermoFisher Scientific (Massachusetts, USA, siRNA ID s599 and s30515, respectively).

Trapped in Agarose DNA Immunostaining (TARDIS) assay.

K562 cells were seeded at a density of 2×10^5 cells/mL and incubated overnight before drug treatment. In experiments measuring the reduction of complexes following etoposide removal from the media, the signal at t_0 needed to be high enough to generate an adequate signal to noise ratio. For this reason, cells were exposed to 100µM etoposide for 2 hours. This is higher than the C_{max} in patient sera (Liston and Davis, 2017), but lower than the 250µM etoposide used in (Ban *et al.*, 2013). TARDIS analyses were performed essentially as described previously (Willmore *et al.*, 1998; Cowell and Austin, 2018; Cowell *et al.*, 2019). TOP2 covalent DNA complexes were visualised by immunofluorescence using primary antibodies for TOP2 (4566-TOP2A and 4555-TOP2B, in-house antibodies raised to the C terminal domain of human TOP2A and TOP2B, respectively (Atwal *et al.*, 2019)) or ubiquitin (FK2, APU2 and

118893

APU3, Merck Millipore) and Alexa -488 or -594 coupled secondary antibodies (anti-rabbit #A11008, or anti-mouse #A11005, ThermoFisher Scientific. UK). Slides were counterstained with the DNA stain Hoechst 33258. Hoechst and AlexaFluor images were captured using an epifluorescence microscope (Olympus IX-81) fitted with an Orca-AG camera (Hamamatsu) and suitable narrow band filter sets employing a 10X objective. Slides were scored automatically as described previously (Atwal *et al.*, 2019) using Volocity 6.3 software (PerkinElmer Inc.). Data were subsequently represented, and statistical analysis was performed using GraphPad Prism 8.2 (Perkin Elmer, San Diego, CA). At least three replica experiments were performed for each TARDIS analysis. For each treatment, median integrated fluorescence values per nucleus were calculated, and these medians were then converted to a percentage of the median obtained for 100 μ M etoposide. For Figures 1, 2, and 5B a separate 100 μ M treatment was included with each replicate for normalisation; for Fig 5A normalisation was performed using the mean value of the medians obtained for 100 μ M etoposide treatment alone. For bar charts the mean \pm SD of the mean of the median values was calculated.

γ H2AX immunofluorescent assays

K562 cells were seeded at a density of 2×10^5 cells/mL and incubated overnight. After drug treatment, cells were washed in PBS and allowed to adhere onto poly-L-lysine coated microscope slides followed by fixation in 4% paraformaldehyde. Cells were permeabilised in KCM-T buffer (120mM KCl, 20mM NaCl, 10mM Tris-HCl pH8.0, 1mM EDTA, 0.1% Triton X-100) and blocked overnight (KCM-T + 2% BSA and 10% dried milk powder). Immunofluorescence staining was performed using anti-phospho-H2AX (Ser139) antibody (Merck Millipore, Massachusetts, USA) and Alexa 594-coupled secondary antibody (anti-mouse, A11005 prior to mounting with Vectashield with DAPI

118893

(Vector Laboratories, Burlingame, CA). Quantitative immunofluorescence and subsequent data analysis was performed as for the TARDIS assay.

Western blotting

After drug treatment or siRNA knockdown, cells were washed in PBS and stored at -80°C until required. Whole cell extracts were prepared by SDS/DNase I extraction as previously described by (Mirski *et al.*, 1993), and western blotting performed by standard methods. Blots were probed with the following antibodies: anti-ubiquitin clone FK2 antibody (1:1000, Merck Millipore), APU2 anti-K48 linked ubiquitin (1:1000, Merck Millipore) anti-UAE1 (Abcam, Cambridge, UK), anti-UBA6 (ThermoFisher) or anti-actin (Abcam). Blots were developed on film or using the LI-COR C-DiGit Chemiluminescence Western Blot Scanner.

Growth inhibition assays

Growth inhibition assays were performed in Nalm-6 cells, as both a wildtype Nalm-6 cell line and a Nalm-6 cell line lacking TOP2B (Nalm-6^{TOP2B-/-}) were available. It was suggested in a previous publication that PRT4165 increases the potency of teniposide specifically via TOP2A (Alchanati *et al.*, 2009), and therefore this allowed us to determine the effect of PRT4165 in cells expressing only TOP2A. Growth inhibition assays were carried out following five days continuous drug exposure, therefore low concentrations of drug need to be used.

Cells were seeded in 96 well plates and incubated at 37 °C, 5% CO₂ for 24 h prior to drug treatment (10,000 cells per well). Cells were then treated with varying concentrations of etoposide alone or in combination with a fixed concentration of the UAE inhibitor MLN7243 or BMI1 inhibitor PRT4165 and incubated for 120 h. After five

118893

days of continuous drug exposure 50 μ l XTT reagent (50:1 XTT reagent to electron coupling reagent, XTT Cell Proliferation kit, Roche, UK) was added per well and cells were incubated at 37 °C for a further 4 h. Absorbance values were obtained using the Bio-Rad 550 Microplate Reader (Bio-Rad, USA) and analysed using GraphPad Prism software (GraphPad Software, USA), version 8. Growth inhibition values were determined by setting the values obtained with no drug as 100% for the etoposide-alone data and with MLN7243/ PRT4165 alone as 100% for the etoposide plus MLN7243/ PRT4165 data.

The IC₅₀ values (concentration at 50% growth inhibition) of etoposide alone versus IC₅₀ of drug in combination with UAE or BMI1 inhibitor were used to calculate potentiation factors (Pf₅₀). The inhibitory concentration of TOP2 poison in the presence of UAE or BMI1 inhibitor was divided by the concentration of TOP2 poison alone for each separate experiment.

Data analysis

Statistical analysis was performed using Graph Pad Prism 8. The details of tests performed are given in figure legends. 2-way ANOVA analysis was non repeated measures. For signifying *P* values, * refers to $P < 0.05$, ** refers to $P < 0.01$, *** refers to $P < 0.001$ and **** refers to $P < 0.0001$. Error bars in bar charts represent SD values. Sample sizes (numbers of replicate experiments) were specified in advance of data acquisition based on prior knowledge of the characteristics of the assays involved and anticipating occasional lost or failed samples. For Fig. 6 data are presented as growth curves with each point representing the mean \pm SEM from replica values.

Results

Effect of the ubiquitin activating enzyme (UAE) inhibitor MLN7243 on levels of TOP2-DNA complexes

In order to investigate the requirement for ubiquitination in the removal of etoposide-induced TOP2A- and TOP2B- DNA complexes, K562 cells were treated with the ubiquitin activating enzyme (UAE) inhibitor, MLN7243 (Misra *et al.*, 2017; Hyer *et al.*, 2018). The conjugation of the 76 amino acid protein ubiquitin to the target protein lysine occurs in a sequential manner involving an E1 ubiquitin activating enzyme (UAE), E2 conjugating enzyme and an E3 ligating enzyme. The first step requires the activation of ubiquitin, which involves the formation of a high energy thioester bond between ubiquitin and ubiquitin activating enzyme (UAE1 or UBA6 in human cells) (Groettrup *et al.*, 2008), and therefore the E1 inhibitor MLN7243 inhibits all ubiquitination. The effect of UAE inhibition on the removal of etoposide-induced TOP2-DNA complexes was examined using the TARDIS assay.

Drug-stabilised TOP2A- and TOP2B- DNA complexes induced in cells can be visualised and quantified using the TARDIS assay, and the kinetics of removal of these complexes can be measured following drug washout. Once in drug free media some TOP2-DNA complexes will be resealed by completion of the enzymes reaction cycle. Those complexes that are not spontaneously reversed require repair processes. Consistent with other studies (Mao *et al.*, 2001; Zhang *et al.*, 2006; Fan *et al.*, 2008; Alchanati *et al.*, 2009; Sunter *et al.*, 2010), we previously demonstrated that efficient repair of TOP2 complexes on chromatin is partly dependent on proteasomal activity

118893

(Lee *et al.*, 2016). This approach was used to address the role of ubiquitin in the processing of etoposide-induced TOP2-DNA complexes. In the TARDIS assay, drug-treated cells are mixed in agarose and spread onto microscope slides. The embedded cells are then lysed in buffer containing SDS and high salt, removing all non-covalently bound proteins and leaving behind only covalently bound TOP2 on genomic DNA in the presence of etoposide (Cowell *et al.*, 2011). TOP2-DNA complexes are then visualised by immunofluorescence.

K562 cells were treated for 2 hours with 100 μ M etoposide (VP-16) alone or in combination with 10 μ M MLN7243 (a specific UAE inhibitor) (Misra *et al.*, 2017; Hyer *et al.*, 2018), or 10 μ M of the proteasome inhibitor MG132. After 2 hours, the culture medium was removed and replaced with etoposide-free medium containing DMSO, MLN7243 or MG132 in order to maintain inhibition of ubiquitination or the proteasome, respectively. The TARDIS assay was used to measure levels of TOP2A- and TOP2B-DNA complexes following 2 hours continuous exposure to etoposide (0 hours after etoposide removal) and after 0.5, 1 and 2 hours incubation in etoposide-free medium.

As previously observed, TOP2A and TOP2B complex levels were both dramatically increased after 2 hours exposure to 100 μ M etoposide compared to untreated cells. Neither MG132 nor MLN7243 resulted in TOP2-DNA complex formation on their own, nor did they significantly affect the accumulation of TOP2 complexes during the 2 hour continuous etoposide incubation (Figure 1A&B). Consistent with previous observations (Lee *et al.*, 2016), etoposide-induced TOP2A- and TOP2B- DNA complex levels fell to less than 25% of the original levels 2 hours after etoposide removal. However, levels of remaining TOP2A-DNA complexes were higher in the presence of 10 μ M MG132. This was statistically significant at 0.5, 1 and 2 hours after

118893

etoposide washout ($p < 0.05$). Remaining TOP2B-DNA complexes were significantly higher at 0.5 hours after etoposide removal in the presence of MG132 compared to cells treated with etoposide alone ($p < 0.001$). This is consistent with the shorter half-life of the TOP2B complexes following removal from drug-containing media (Willmore *et al.*, 1998). Incubation of cells with 10 μ M MLN7243 also slowed the removal of etoposide-induced TOP2A- and TOP2B- DNA complexes, similarly to proteasome inhibition. Levels of remaining TOP2A-DNA complexes were significantly higher at 0.5, 1 and 2 hours after etoposide washout ($p < 0.05$, < 0.001 and < 0.001 , respectively), and TOP2B-DNA complexes were significantly higher after 0.5 hours ($p < 0.001$). To determine whether the effects of MG132 and MLN7243 are epistatic, cells treated with etoposide were also co-treated with both MG132 and MLN7243. When both inhibitors were administered together, the levels of etoposide-induced TOP2A- and TOP2B-DNA complexes that accumulated during the 2 hour incubation were significantly increased ($p < 0.01$ and 0.001 , respectively). However, no additive effect was observed on the rate of removal of TOP2A or TOP2B complexes when both inhibitors were administered together with etoposide compared to each inhibitor alone. This suggests that both inhibitors exert their effects via the same pathway, and that the route to proteasomal degradation of etoposide-induced TOP2-DNA complexes is ubiquitin-dependent as it requires E1 ubiquitin activating enzyme activity. Even in the presence of MG132 and / or MLN7243 the complex levels eventually return to background levels, but more slowly. This suggests that the proteasomal repair pathway is probably not the only pathway for repair of the TOP2-DNA complexes. Attempts at estimating the proportion of TOP2-DNA complexes processed via a ubiquitin-dependent route are complicated by fact that these complexes resolve after etoposide washout through the combined effect of one or more repair/processing pathways, together with

118893

spontaneous reversal of the complexes by completion of the enzymes reaction cycle following removal of etoposide. From the data in Fig.1, MLN7243 results in approximately 20% and 100% additional retention of TOP2A one and two hours after etoposide washout respectively (in relation to the signal for each treatment at the time of drug washout). Thus, at later time points at least, a substantial proportion (up to 50%) of the removal of TOP2A complexes appears to be ubiquitin dependent. The overall reversal rate is faster for TOP2B, and 30 minutes after etoposide washout MLN7243 results in approximately 50% additional retention compared to the DMSO control. Thus, a substantial proportion (approximately a third) of the disappearance of TOP2B complexes appears to be attributable to a ubiquitin-dependent mechanism.

Figure 1C shows western blots probed with antibody FK2 which detects all ubiquitin conjugates. Inhibition of the proteasome by MG132 increased the amount of ubiquitin conjugates detected. In contrast, ubiquitinated conjugates were absent following inhibition with 10 μ M MLN7243 (even in the presence of MG132, Figure 4A), confirming potent inhibition of ubiquitination.

The specificity of MLN7243 for ubiquitin E1 enzymes was recently demonstrated by (Misra *et al.*, 2017), and thus the effect of MLN7243 on levels of TOP2-DNA complexes is unlikely to be due to off-target effects. Indeed, removal of TOP2A-DNA complexes was also decreased by another structurally distinct UAE inhibitor, PYR-41 (Supplemental Fig.1A). TARDIS experiments were performed following the co-treatment of cells with or without 50 μ M PYR41. At this concentration, PYR-41 reduces levels of ubiquitin conjugates even in the presence of MG132 (as measured by western blotting, Supplemental Fig. 1B) and significantly reduced TOP2A complex

118893

resolution at 30 and 60 minutes after removal of etoposide (Supplemental Fig.1A). For TOP2B, complex levels were significantly increased at t0 (2 hours treatment with etoposide) and remained significantly higher than the non-PYR41 treated cells 30 minutes after etoposide removal. To test the possibility that this effect is due to non-specific inhibition of other ubiquitin-like E1 enzymes, the TARDIS assay was performed in the presence and absence of the highly specific Nedd8 activating enzyme (NAE) inhibitor, MLN4924. Neddylation is required for the ubiquitination of proteins by a specific class of E3 ubiquitin ligases (the cullin-RING family). However, MLN4924 did not affect the levels of etoposide-induced TOP2-DNA complexes following removal of etoposide. The TARDIS data is shown as scatter plots in Supplemental Figure 2 and suggests the effect of MLN7243 is not due to non-specific inhibition of NAE.

Furthermore, MLN7243 treatment did not affect levels of SUMOylated TOP2-DNA complexes, as measured by TARDIS assay (Supplemental Fig 3) indicating MLN7243 does not inhibit SAE at the concentration used in this assay.

Ubiquitination is required for the appearance of etoposide induced DSBs

The degradation of TOP2-DNA complexes by the proteasome leads to the appearance of protein-free DSBs which are otherwise concealed by TOP2 protein and which result in S-139 phosphorylation of histone H2AX (Zhang *et al.*, 2006; Zhao *et al.*, 2006; Lyu *et al.*, 2007; Fan *et al.*, 2008). The specificity of H2AX phosphorylation for DSBs in this setting is supported by the previous observations that H2AX phosphorylation mirrors DSB break induction measured by other means (alkaline Comet or constant field gel electrophoresis) (Smart *et al.*, 2008; Muslimović *et al.*, 2009) and that the disappearance of etoposide-induced γ H2AX foci after treatment is delayed in cells

118893

treated with the DSB repair inhibitor NU7411 and in NHEJ-deficient *LIG4* null cells (Riballo *et al.*, 2004; Zhao *et al.*, 2006). To determine whether the appearance of etoposide-induced DSBs is also dependent on E1 activity, the γ H2AX assay was used to measure levels of TOP2-free DSBs after etoposide treatment alone or in combination with the E1 inhibitor, MLN7243, or the proteasome inhibitor MG132. As previously reported (Zhang *et al.*, 2006; Fan *et al.*, 2008; Tammaro *et al.*, 2013), co-incubation with MG132 reduced the appearance of the etoposide-induced γ H2AX signal (Figure 2A) which was statistically significant after 2 and 4 hours of drug treatment ($p < 0.001$ and 0.001) where γ H2AX signal was reduced by approximately 50%. Notably, etoposide-induced γ H2AX levels remained significantly above background even in the presence of MG132, consistent with the presence of alternative proteasome-independent mechanisms of TOP2-DNA complex processing to DSBs.

γ H2AX levels were also reduced in the presence of the E1 inhibitor MLN7243 compared to etoposide alone (Figure 2B, 2C), and this was statistically significant at all time points tested ($p < 0.05$). In addition to continuous exposure to etoposide for 1, 2 or 4 hours, we also included a 2 hour etoposide treatment followed by etoposide removal and 2 hours incubation in etoposide-free medium or medium containing MLN7243 (2+2hr washout, WO). This is equivalent to the two hour time point (t_2) in the TARDIS assay in Figure 1 and the 2 hour continuous exposure is equivalent to the t_0 in the TARDIS assay in Figure 1. To test whether the effect of UAE inhibition was specific to etoposide-induced DNA damage, the γ H2AX assay was performed following X-ray irradiation in the presence and absence of the E1 inhibitor MLN7243. IR-induced γ H2AX levels were not reduced in the presence of the E1 inhibitor MLN7243 (Figure 2D). Conversely, γ H2AX levels were slightly increased by E1

118893

inhibition 4 hours after irradiation ($p < 0.01$), consistent with inhibition of DNA repair (Moudry *et al.*, 2012). This shows that ubiquitination is not required for the phosphorylation of histone H2AX but is involved specifically in the appearance of topoisomerase mediated DSBs following etoposide exposure.

siRNA knockdown of ubiquitin activating enzymes

The role of ubiquitin in the removal of etoposide induced TOP2-DNA complexes was also investigated following siRNA knockdown of UAE1 and UBA6. This did significantly reduce the appearance of etoposide-induced γ H2AX signal following continuous etoposide exposure, albeit to a lesser degree than was observed with MG132 or MLN7243 (Figure 2E & 2F). Phosphorylation of histone H2AX was still detectable following UAE1 and UBA6 knockdown, reflecting other ubiquitin-independent mechanisms of TOP2-DNA complex removal or incomplete suppression of E1 activity by these siRNAs.

The TARDIS assay was also performed on siRNA knockdown cells (UAE1 siRNA) to measure levels of etoposide induced TOP2A- and TOP2B- DNA complexes compared to control cells transfected with non-silencing siRNA (CON siRNA). Levels of TOP2B-DNA complexes were significantly increased in UAE1 siRNA knockdown cells following 2 hours of exposure to etoposide ($p < 0.001$, Figure 3A). However, unlike E1 inhibition with MLN7243 (Fig. 1), levels of TOP2A-DNA complexes were not significantly affected by siRNA knockdown of the E1 ubiquitin activating enzyme UAE1 (Fig. 3A), despite efficient UAE1 silencing (Fig 3B). In addition, TOP2A- and TOP2B-DNA complexes returned to background levels following the removal of etoposide, regardless of UAE1 knockdown. This could be due to residual UAE1 activity or the activity of the second and more recently discovered UAE enzyme, UBA6 (Groettrup *et*

118893

al., 2008). However, the removal of etoposide-induced TOP2-DNA complexes was also unaffected by UBA6 siRNA or double siRNA knockdown of UAE1 and UBA6 (Supplemental Figure 4A and B). The scatter plots shown in supplemental Figure 4 show the signal from individual cells and the numbers of cells analysed is shown above each column. The knockdown by UAE1 siRNA is shown in Figure 3B, and the knockdown by UBA6 and the double knockdown are shown in Supplemental Figures 4C and 4D.

It is unclear why siRNA-mediated depletion of UAE significantly reduces levels of etoposide-induced H2AX phosphorylation but not the resolution of TOP2-DNA complexes observed using the TARDIS assay. However, several factors may contribute to this apparent discrepancy. Firstly, spontaneous reversal is a major contributor to complex resolution upon etoposide washout (see above). This could mask a small effect of UAE depletion on TOP2 complex processing as observed in the TARDIS assay. In contrast, H2AX phosphorylation occurs as a result of processing to protein-free breaks and so would be expected to be more sensitive to modest changes in processing efficiency. Secondly, the γ H2AX assay simultaneously measures the processing of both TOP2A and TOP2B complexes while the TARDIS assay is isoform specific. Thus, small differences with UAE knockdown may be more readily detectable in the γ H2AX assay due to the combined effects of both isoforms. Thirdly, while we measure loss of the original TOP2-DNA complex signal over a period of 2 hours using the TARDIS assay, the γ H2AX assay was used to quantify the accumulation of signal over time. So, at longer time points (1 or 2 hours) there is a reducing signal to noise ratio for the TARDIS assay, but a robust and increasing signal for the H2AX assay. Notably, the two hours of etoposide incubation in the γ H2AX assays shown in Fig. 2E is equivalent to the zero-hour washout the TARDIS experiments in Fig. 3A. At this time

118893

point, more TOP2B complexes are retained in the siRNA depleted TARDIS sample which is consistent with the reduction in H2AX signal observed in the siRNA-treated cells.

Differences between siRNA knockdown and small molecule inhibitor approaches may also be explained by incomplete knockdown of E1 activating activity with siRNA. To test the effectiveness of the siRNA knockdown on protein ubiquitination, a ubiquitination assay was performed to compare levels of remaining E1 activity in siRNA knockdown cells with MLN7243-treated cells. Despite efficient siRNA-mediated silencing of UAE1 and UBA6 E1 proteins determined by western blotting (Figure 3B and Supplemental Figure 4 C & D), some ubiquitination activity remained detectable in UAE1/UBA6 siRNA treated cells, evidenced by the presence of ubiquitinated proteins in whole cell extracts by western blotting with antibody FK2 (Figure 4A). Upon treatment with a proteasome inhibitor, there is an accumulation of ubiquitinated proteins which would otherwise be degraded by the proteasome. This was evident in control cells treated with MG132 for 2 hours compared to the DMSO control (Figure 4A, compare lane 1 with lane 2 and lane 5 with lane 6). Although the MG132-induced accumulation of ubiquitinated proteins was reduced in UAE1/UBA6 knockdown cells (Lane 4), it was not eliminated. In contrast, there was no detectable accumulation of ubiquitinated proteins in MLN7243-treated cells (lane 7), consistent with complete E1 inhibition. Thus, under the conditions employed ubiquitination activity was more robustly inhibited by chemical inhibition of UAE with MLN7243 than by UAE1/UBA6 siRNA knockdown.

118893

Investigating TOP2 ubiquitination using the TARDIS assay

The role of ubiquitin in the removal of TOP2-DNA complexes could involve the direct ubiquitination of TOP2 or the modification of other proteins involved in processing. To investigate this further, ubiquitination of the TOP2 trapped in DNA complexes was examined by TARDIS assay

The TARDIS assay was adapted to study the post-translational modification of TOP2-DNA complexes by probing with anti-ubiquitin antibodies. During TARDIS slide processing, cells are lysed in buffer containing 1% SDS and 1M NaCl which removes all non-covalently bound proteins from DNA. This includes histones and other proteins tightly associated with chromatin, such as RNA polymerase II and Ku80, confirmed by probing TARDIS slides for histones, RNA polymerase II and KU antigen (Supplemental Figure 5). Ubiquitin TARDIS detects ubiquitin on the TOP2 which is covalently bound to DNA in TOP2-DNA complexes. Levels of conjugated ubiquitin on the TOP2-DNA covalent complexes were measured using the FK2 antibody in TARDIS, and the signal was detectable following 2 hours etoposide exposure (Figure 4B&C, Supplementary Figure 6). This demonstrates that TOP2-DNA complexes are ubiquitinated. Levels of ubiquitin conjugates were reduced to background levels when cells were co-incubated with E1 inhibitor MLN7243 (Figure 4B). Levels of ubiquitinated TOP2-DNA complexes were also reduced in UAE1/UBA6 siRNA knockdown cells but remained significantly above background levels (Figure 4C), consistent with the siRNA knockdown of E1 activity being incomplete as shown in Figure 4A. Notably, these differences were not due to reduced levels of TOP2A- or TOP2B- DNA complexes, as neither MLN7243 treatment nor UAE1/UBA6 siRNA knockdown reduced levels of

118893

TOP2-DNA complexes following 2 hours continuous etoposide exposure when measured by TARDIS assay (see Figs 1&3 and Supplemental Figure 4, respectively).

TARDIS slides were also probed with linkage-specific ubiquitin antibodies which detect K48- and K63- linked polyubiquitin chains. Low levels of both K48- and K63-linked ubiquitin were detected in etoposide-treated cells (Supplemental Figure 6), which are typically associated with proteasomal degradation and signalling pathways, respectively.

Use of the TARDIS assay to study the role of BMI1/RING1A E3 ubiquitin ligase in the processing of etoposide-induced TOP2-DNA complexes

BMI1/RING1A is an E3 ubiquitin ligase previously implicated in the teniposide-induced proteasomal degradation of TOP2A-DNA complexes (Alchanati *et al.*, 2009). In the current study, the role of BMI1/RING1A in the processing of etoposide induced TOP2-DNA complexes was investigated using the TARDIS assay and the BMI1/RING1A inhibitor, PRT4165 (Alchanati *et al.*, 2009; Ismail *et al.*, 2013). K562 cells were treated with 100 μ M etoposide alone or in combination with 90 μ M PRT4165 for 2 hours, followed by incubation in etoposide-free medium containing DMSO or PRT4165 to maintain inhibition of BMI1/RING1A. Cells were collected 0, 0.5, 1 and 2 hours after etoposide removal, and levels of TOP2A- and TOP2B-DNA complexes were measured using the TARDIS assay. Levels of TOP2A- and TOP2B- DNA complexes were not significantly affected following 2 hours continuous exposure to etoposide (Figure 5A). However, levels of remaining TOP2A-DNA complexes were significantly higher in the presence of PRT4165 following 30 minutes or 60 minutes incubation in etoposide-free medium ($p < 0.001$), consistent with a role for BMI1/RING1A in the processing of TOP2A-DNA complexes. Levels of remaining TOP2B-DNA complexes

118893

were also significantly higher in PRT4165-treated cells 30 minutes and 60 minutes after etoposide removal ($p < 0.05$). This suggests that BMI1/RING1A is involved in the removal of both TOP2A- and TOP2B- complexes from DNA.

To test the effect of PRT4165 on the ubiquitination of TOP2-DNA complexes, the ubiquitin TARDIS assay was performed in K562 cells treated with 100 μ M etoposide alone or in combination with 90 μ M PRT4165. As shown in Figure 5B, levels of etoposide-induced ubiquitinated TOP2-DNA complexes were significantly reduced in the presence of PRT4165, suggesting BMI1/RING1A is involved in the ubiquitination of TOP2.

The effect of PRT4165 on the processing of etoposide-induced TOP2-DNA complexes was also investigated using the γ H2AX assay. K562 cells were treated with 100 μ M etoposide alone or in combination with 90 μ M PRT4165 for up to 4 hours and DSB levels were measured after 0, 1, 2- and 4-hours continuous drug exposure. The appearance of etoposide induced DSBs was significantly reduced in the presence of PRT4165 at all time points tested ($p < 0.001$, Figure 5C), suggesting the ubiquitin-dependent processing of etoposide-induced TOP2-DNA complexes to DSBs is largely BMI1/RING1A-dependent.

Effect of UAE inhibition on the growth-inhibitory effects of etoposide

To investigate the effect of UAE inhibition on the growth inhibitory effects of the TOP2 poison etoposide, growth inhibition assays (XTT) were first used to determine the IC₂₀ (concentration at 20% growth inhibition) of MLN7243 in Nalm-6 cells. For Nalm-6 cells the IC₂₀ of MLN7243 was 400 nM.

118893

To examine the effect of MLN7243 on the growth inhibitory effects of etoposide, Nalm-6 wild type cells were treated with increasing concentrations of etoposide alone or in combination with 400 nM MLN7243. The effect of MLN7243 on the growth inhibitory effects of each TOP2 poison was quantified by a potentiation factor (Pf_{50}), which was calculated as a ratio of the IC_{50} of TOP2 poison alone and the IC_{50} of TOP2 poison in combination with MLN7243. Potentiation was deemed statistically significant if there was a significant difference between the IC_{50} of TOP2 poison alone versus IC_{50} of TOP2 poison in combination with MLN7243, as determined by an unpaired t-test. Strikingly, co-incubation of Nalm-6 cells with MLN7243 significantly reduced the IC_{50} of etoposide ($P<0.001$), resulting in a Pf_{50} of 3.1.

To investigate the role of TOP2B in the potentiation of etoposide with MLN7243, growth inhibition assays were repeated in Nalm-6^{TOP2B-/-} cells. Nalm-6^{TOP2B-/-} cells were treated with increasing concentrations of etoposide for 120 hours, alone or in combination with 400 nM MLN7243. MLN7243 significantly reduced the IC_{50} of etoposide from 169 nM to 104.33 nM in the presence of MLN7243, giving a Pf_{50} of 1.63 ($p=0.0001$). The Pf_{50} value for etoposide was significantly smaller in Nalm-6^{TOP2B-/-} cells compared to the Pf_{50} value of 3.1 in Nalm-6 wild type cells. This suggests that the potentiation of MLN7243 is mediated by both TOP2A and TOP2B.

Effect of BMI1/RING1A inhibition on the growth-inhibitory effects of TOP2 poison etoposide

PRT4165 is a small molecule inhibitor of the E3 ubiquitin ligase BMI1/RING1A which was shown to inhibit the etoposide-induced degradation of TOP2A-DNA complexes and the auto-ubiquitination of BMI1/RING1A (Alchanati *et al.*, 2009) and which we

118893

have demonstrated also inhibits the processing of both TOP2A and TOP2B DNA complexes (Fig.5A&C). The IC₂₀ of PRT4165 was determined to be to be 35 μ M for Nalm-6 cells. Incubation of cells with PRT4165 at this concentration significantly reduced the IC₅₀ of etoposide ($p < 0.05$) with a Pf₅₀ value of 1.5. This shows that the growth inhibitory effect of etoposide can be increased by inhibition of the BMI1/RING1A ubiquitin ligase. In order to examine the role of each TOP2 isoform in the potentiation of TOP2 poisons with PRT4165, growth inhibition assays were also performed in Nalm-6^{TOP2B-/-} cells. PRT4165 potentiation of etoposide remained significant ($p < 0.05$) with a Pf₅₀ of 1.6 in Nalm-6^{TOP2B-/-} cells. The very similar Pf₅₀ values observed in WT and TOP2B null Nalm-6 cells suggests that potentiation of etoposide by PRT4165 operates largely via TOP2A. This is consistent with the finding of Alchanati et al, whereby BMI1/RING1A silencing reduced drug-induced TOP2A degradation, but was not predicted from the finding that PRT4165 inhibits the processing of both TOP2A and TOP2B complexes (Fig. 5). This apparent inconsistency could be explained by the different conditions under which the assays are performed. For growth inhibition assays, cells were exposed continuously for five days to etoposide up to 300nM (i.e. several times the IC₅₀ value) while for TOP2 complex reversal assays (TARDIS) cells were exposed over a shorter course to a much higher etoposide concentration (100 μ M, necessary to induce a robust signal for quantification of complex reversal). Thus, a caveat of this study is that the conditions for measuring complex reversal and cell sensitization are not equivalent. We hypothesize that under the conditions used for growth inhibition assays, PRT4165 sensitises cells to etoposide largely via inhibition of TOP2A-DNA complex processing, consistent with the TOP2A-specific effect reported by (Alchanati *et al.*, 2009) whereas in TARDIS assays we are able to detect an effect on both TOP2 isoforms, perhaps

118893

due to the much larger accumulation of TOP2-DNA complexes. However, it should be noted in the Alchanati study the cells were incubated in drug free media for 30 minutes prior to the detection of complexes and the TOP2B complex half-life is shorter than that of TOP2A. Notably, the degree of potentiation is similar for PRT4165 and MLN7243 in TOP2B null cells (Fig. 6 B&D). This suggests that under growth inhibition conditions the effect of MLN7243, but not PRT4165 is significantly dependent on TOP2B, consistent with a general effect on proteasomal processing of TOP2 complexes resulting from E1 inhibition, but a more specific effect on TOP2A with BMI1/RING1A inhibition.

Discussion

The repair of drug-stabilised TOP2-DNA complexes is particularly challenging due to the covalent attachment of TOP2 to DNA. Among other mechanisms, TOP2 can be removed from the TOP2-DNA complex by proteasomal degradation (Mao *et al.*, 2001; Zhang *et al.*, 2006; Fan *et al.*, 2008; Lee *et al.*, 2016), and the remaining 5'-phosphotyrosine adduct may then be hydrolysed by the 5'-phosphodiesterase, TDP2 (Cortes Ledesma *et al.*, 2009; Zeng *et al.*, 2011; Schellenberg *et al.*, 2012; Gao *et al.*, 2014). This culminates in the liberation of protein-free DNA ends that result in a DNA damage response including phosphorylation of histone H2AX (Gittens *et al.*, 2019; Gothe *et al.*, 2019) and are a substrate for NHEJ repair (Mårtensson *et al.*, 2003; Malik *et al.*, 2006; Maede *et al.*, 2014). Ubiquitination has been reported to play a role in the removal of stalled TOP2 complexes on DNA.

118893

Ubiquitin itself contains seven lysine residues which can be ubiquitinated, forming polyubiquitin chains (Komander, 2009). The conjugation of ubiquitin to target proteins requires multiple enzymatic steps, firstly involving an E1 ubiquitin activating enzyme (UAE1 or UBA6), then an E2 conjugating enzyme and finally an E3 ligating enzyme. The key first step is the activation of ubiquitin which involves the formation of a high energy thioester bond between ubiquitin and ubiquitin activating enzyme (UAE1 or UBA6 in human cells) (Groettrup *et al.*, 2008). Thus, the UAE small molecular inhibitor MLN7243 inhibits all ubiquitination. Previous studies on the role of E1 in the processing of TOP2-DNA complexes have utilised a murine cell line with a temperature sensitive E1; however, two studies using this cell line reported different results regarding its role in the processing of epipodophyllotoxin-induced TOP2-DNA complexes. Both previous studies utilised western blotting to determine the levels of TOP2 under various conditions, which allows only the measurement of pooled protein populations including both unbound TOP2 and TOP2 in TOP2-DNA complexes in a manner that is difficult to quantify. While data in the first study suggested that the proteasomal degradation of TOP2B was ubiquitin dependent, the second study proposed a ubiquitin-independent mechanism of TOP2B proteasomal degradation following etoposide treatment, involving the collision of drug-stabilised TOP2B-DNA complexes with elongating RNA polymerase II. In this model, the proteasome was suggested to be recruited to the trapped TOP2B-DNA complex by RNA pol II-associated 19S AAA ATPases (Ban *et al.*, 2013). Thus the requirement for ubiquitin in the degradation of TOP2B-DNA complexes has remained unclear (Mao *et al.*, 2001; Ban *et al.*, 2013).

118893

A major aim of the current study was therefore to clarify inconsistencies in the literature regarding the role of the E1 ubiquitin activating enzyme in the removal of TOP2 complexes following drug exposure. To do this, a combination of small molecule inhibitor and siRNA knockdown approaches were used. Supra-clinical concentrations of etoposide (100 μ M) were used to ensure our data was comparable to previous studies in which concentrations of up to 250 μ M etoposide were used. High concentrations of etoposide were also required to generate a robust signal in the TARDIS assay, which would otherwise become undetectable and unquantifiable with time following etoposide removal from the cell culture media. While the use of high etoposide concentrations was necessary to address the aims of this study, it is important to note that circulating concentrations of etoposide in clinical use are much lower than 100 μ M. A C_{\max} of 33 μ M is cited in a review by (Liston and Davis, 2017) and, depending upon the regime, much lower concentrations of etoposide may be present in patient sera. Lower etoposide concentrations (up to 0.3 μ M) were used in the five day growth inhibition assays shown in Figure 6.

The effect of UAE inhibition by MLN7243 on the removal of etoposide-induced TOP2-DNA complexes was examined using the TARDIS assay, allowing quantitative measurement of TOP2-DNA complex removal on a cell-by-cell basis (Fig. 1 and Supplemental Figure 1). Inhibition of UAE reduced the removal of etoposide-stabilised TOP2-DNA covalent complexes to a similar degree as proteasomal inhibition with MG132, consistent with a role for ubiquitination in the removal of TOP2 complexes. Indeed, combination experiments with MLN7243 and MG132 suggest that the ubiquitin-dependent pathway is epistatic with the proteasomal processing pathway. In

118893

addition, processing of the TOP2-DNA complexes to frank DSBs (detectable by γ H2AX assay) was also inhibited by MLN7243, and comparable to the effect of inhibition of the proteasome by MG132, further suggesting that they are part of the same pathway (Figure 2A and B). Processing of TOP2-DNA complexes to DSBs was also reduced by siRNA knockdown of E1 enzymes (Fig. 2E&F). As alluded to above, there have been conflicting reports regarding the requirement for protein ubiquitination in the resolution of TOP2 poison-induced TOP2-DNA complexes (Mao *et al.*, 2001; Ban *et al.*, 2013). However, the experiments reported here employing pharmacological inhibition and siRNA knockdown of UAE activity strongly support a ubiquitin dependent component to the processing of TOP2-DNA covalent complexes to DSBs that evoke a DNA damage response.

We have shown that ubiquitin is required for efficient processing of TOP2-DNA complexes to protein-free DSBs and protein ubiquitination is therefore an important layer of regulation in the repair of TOP2 poison-induced DNA damage. We also show that at least some etoposide-induced TOP2-DNA complexes are conjugated with ubiquitin. However, an important limitation of the ubiquitin TARDIS assay is that it does not reveal the ubiquitination status of TOP2 protein that is not covalently bound to DNA (before the addition of etoposide). Therefore, we were not able to determine whether the observed TOP2 ubiquitination occurs as a consequence of TOP2 poisoning or represents a constitutive level of TOP2 ubiquitination. Similarly, although the simplest explanation for the ubiquitin dependence of TOP2-DNA complex processing is a requirement for conjugation of ubiquitin to TOP2, we cannot exclude alternative explanations including ubiquitination of another protein that is required for efficient TOP2-DNA complex processing.

118893

It is also important to note that, like UAE inhibition, proteasomal inhibition is reported to deplete levels of nuclear ubiquitin (Xu *et al.*, 2004; Dantuma *et al.*, 2006; Heidelberger *et al.*, 2018). Therefore, we also cannot fully exclude the possibility that the observed proteasome-dependent processing of TOP2-DNA complexes is due to inhibition of another ubiquitin-dependent (but proteasome-independent) pathway.

BMI1/RING1A is an E3 ubiquitin ligase previously implicated in the proteasomal degradation of etoposide-induced TOP2A-DNA complexes (Alchanati *et al.*, 2009). We show here that, like UAE inhibition, inhibition of BMI1/RING1A also reduces the processing of etoposide-induced TOP2A-DNA complexes. We also show that BMI1/RING1A is required for the efficient processing of TOP2B-DNA complexes, indicating a ubiquitin-dependent processing pathway which is common to both TOP2 isoforms. However, as described above, the ubiquitin- and BMI1/RING1A- dependent processing of TOP2-DNA complexes may involve the ubiquitination of TOP2, or alternatively, the modification of another protein involved in TOP2-DNA complex repair. Although PRT4165 inhibited processing of both TOP2A and TOP2B-DNA complexes, growth inhibition experiments in WT and TOP2B null Nalm-6 cells indicated that etoposide potentiation by PRT4165 was largely independent of TOP2B. However, it is important to note that for practical reasons the TARDIS and growth inhibition assays utilised very different etoposide concentrations (100µM vs ≤ 300nM respectively). These data also allow the possibility of at least one other E3 ubiquitin ligase that targets TOP2B, whose contribution may be more significant at lower etoposide concentrations.

Given the clinical interest in the ubiquitin-proteasome system and the ongoing development of specific inhibitors, these results suggest that the therapeutic

118893

cytotoxicity of TOP2 poisons could be enhanced through combination therapy with UAE inhibitors, or by specific inhibition of the BMI1/RING1A ubiquitin ligase which would lead to increased cellular accumulation or persistence of TOP2-DNA complexes. In support of this idea we have shown previously that proteasomal inhibition potentiates the cytotoxicity of TOP2 poisons in a cell culture system (Lee *et al.*, 2016). In the present study we show that co-incubation of etoposide with MLN7243 or PRT4165 potentiates the cytotoxicity of etoposide (Fig. 6). In addition, we hypothesise that reduced conversion of TOP2-DNA complexes to protein-free DNA DSBs may also diminish the occurrence of genotoxic side-effects of TOP2 poisons, including the formation of leukemia-inducing chromosome translocations.

Acknowledgements

Author contributions

Participated in research design: Swan, Cowell, Poh, Austin

Conducted experiments: Swan, Cowell, Poh

Performed data analysis: Swan, Cowell

Wrote or contributed to writing of the manuscript: Swan, Cowell, Austin

The authors declare that they have no conflict of interest.

118893

References

- Alchanati I, Teicher C, Cohen G, Shemesh V, Barr HM, Nakache P, Ben-Avraham D, Idelevich A, Angel I, Livnah N, Tuvia S, Reiss Y, Taglicht D, and Erez O (2009) The E3 ubiquitin-ligase Bmi1/Ring1A controls the proteasomal degradation of Top2alpha cleavage complex - a potentially new drug target. *PLoS ONE* **4**:e8104.
- Aparicio T, Baer R, Gottesman M, and Gautier J (2016) MRN, CtIP, and BRCA1 mediate repair of topoisomerase II–DNA adducts. *J Cell Biol* **212**:399–408.
- Atwal M, Swan RL, Rowe C, Lee KC, Lee DC, Armstrong L, Cowell IG, and Austin CA (2019) Intercalating TOP2 Poisons Attenuate Topoisomerase Action at Higher Concentrations. *Mol Pharmacol* **96**:475–484.
- Azarova AM, Lyu YL, Lin C-P, Tsai Y-C, Lau JY-N, Wang JC, and Liu LF (2007) Roles of DNA topoisomerase II isozymes in chemotherapy and secondary malignancies. *Proc Natl Acad Sci USA* **104**:11014–11019.
- Ban Y, Ho C-W, Lin R-K, Lyu YL, and Liu LF (2013) Activation of a Novel Ubiquitin-Independent Proteasome Pathway when RNA Polymerase II Encounters a Protein Roadblock. *Mol Cell Biol* **33**:4008–4016.
- Cortes Ledesma F, El Khamisy SF, Zuma MC, Osborn K, and Caldecott KW (2009) A human 5'-tyrosyl DNA phosphodiesterase that repairs topoisomerase-mediated DNA damage. *Nature* **461**:674–678.
- Cowell IG, and Austin CA (2018) Visualization and Quantification of Topoisomerase-DNA Covalent Complexes Using the Trapped in Agarose Immunostaining (TARDIS) Assay. *Methods Mol Biol* **1703**:301–316.
- Cowell IG, Ling EM, Swan RL, Brooks MLW, and Austin CA (2019) The Deubiquitinating Enzyme Inhibitor PR-619 is a Potent DNA Topoisomerase II Poison. *Mol Pharmacol* **96**:562–572.
- Cowell IG, Tilby MJ, and Austin CA (2011) An overview of the visualisation and quantitation of low and high MW DNA adducts using the trapped in agarose DNA immunostaining (TARDIS) assay. *Mutagenesis* **26**:253–260.
- Dantuma NP, Groothuis TAM, Salomons FA, and Neefjes J (2006) A dynamic ubiquitin equilibrium couples proteasomal activity to chromatin remodeling. *J Cell Biol* **173**:19–26.
- Errington F, Willmore E, Leontiou C, Tilby MJ, and Austin CA (2004) Differences in the longevity of topo II α and topo II β drug-stabilized cleavable complexes and the relationship to drug sensitivity. *Cancer Chemother Pharmacol* **53**:155–162.
- Fan J-R, Peng A-L, Chen H-C, Lo S-C, Huang T-H, and Li T-K (2008) Cellular processing pathways contribute to the activation of etoposide-induced DNA damage responses. *DNA Repair* **7**:452–463.

118893

- Gao R, Schellenberg MJ, Huang SN, Abdelmalak M, Marchand C, Nitiss KC, Nitiss JL, Williams RS, and Pommier Y (2014) Proteolytic Degradation of Topoisomerase II (Top2) Enables the Processing of Top2-DNA and Top2-RNA Covalent Complexes by Tyrosyl-DNA-Phosphodiesterase 2 (TDP2). *J Biol Chem* **289**:17960–17969.
- Gittens WH, Johnson DJ, Allison RM, Cooper TJ, Thomas H, and Neale MJ (2019) A nucleotide resolution map of Top2-linked DNA breaks in the yeast and human genome. *Nat Commun* **10**:1–16.
- Gothe HJ, Bouwman BAM, Gusmao EG, Piccinno R, Petrosino G, Sayols S, Drechsel O, Minneker V, Josipovic N, Mizi A, Nielsen CF, Wagner E-M, Takeda S, Sasanuma H, Hudson DF, Kindler T, Baranello L, Papantonis A, Crosetto N, and Roukos V (2019) Spatial Chromosome Folding and Active Transcription Drive DNA Fragility and Formation of Oncogenic MLL Translocations. *Mol Cell* **75**.
- Groettrup M, Pelzer C, Schmidtke G, and Hofmann K (2008) Activating the ubiquitin family: UBA6 challenges the field. *Trends Biochem Sci* **33**:230–237.
- Hamilton NK, and Maizels N (2010) MRE11 function in response to topoisomerase poisons is independent of its function in double-strand break repair in *Saccharomyces cerevisiae*. *PLoS ONE* **5**:e15387.
- Hartsuiker E, Neale MJ, and Carr AM (2009) Distinct requirements for the Rad32(Mre11) nuclease and Ctp1(CtIP) in the removal of covalently bound topoisomerase I and II from DNA. *Mol Cell* **33**:117–123.
- Heidelberger JB, Voigt A, Borisova ME, Petrosino G, Ruf S, Wagner SA, and Beli P (2018) Proteomic profiling of VCP substrates links VCP to K6-linked ubiquitylation and c-Myc function. *EMBO Rep* **19**:e44754.
- Hoa NN, Shimizu T, Zhou ZW, Wang Z-Q, Deshpande RA, Paull TT, Akter S, Tsuda M, Furuta R, Tsutsui K, Takeda S, and Sasanuma H (2016) Mre11 Is Essential for the Removal of Lethal Topoisomerase 2 Covalent Cleavage Complexes. *Mol Cell* **64**:580–592.
- Hyer ML, Milhollen MA, Ciavarri J, Fleming P, Traore T, Sappal D, Huck J, Shi J, Gavin J, Brownell J, Yang Y, Stringer B, Griffin R, Bruzzese F, Soucy T, Duffy J, Rabino C, Riceberg J, Hoar K, Lublinsky A, Menon S, Sintchak M, Bump N, Pulukuri SM, Langston S, Tirrell S, Kuranda M, Veiby P, Newcomb J, Li P, Wu JT, Powe J, Dick LR, Greenspan P, Galvin K, Manfredi M, Claiborne C, Amidon BS, and Bence NF (2018) A small-molecule inhibitor of the ubiquitin activating enzyme for cancer treatment. *Nat Med* **24**:186–193.
- Isik S, Sano K, Tsutsui Kimiko, Seki M, Enomoto T, Saitoh H, and Tsutsui Ken (2003) The SUMO pathway is required for selective degradation of DNA topoisomerase II β induced by a catalytic inhibitor ICRF-1931. *FEBS Letters* **546**:374–378.

118893

- Ismail IH, McDonald D, Strickfaden H, Xu Z, and Hendzel MJ (2013) A small molecule inhibitor of polycomb repressive complex 1 inhibits ubiquitin signaling at DNA double-strand breaks. *J Biol Chem* **288**:26944–26954.
- Komander D (2009) The emerging complexity of protein ubiquitination. *Biochem Soc Trans* **37**:937.
- Lee KC, Bramley RL, Cowell IG, Jackson GH, and Austin CA (2016) Proteasomal inhibition potentiates drugs targeting DNA topoisomerase II. *Biochem Pharmacol* **103**:29–39.
- Lee KC, Padget K, Curtis H, Cowell IG, Moiani D, Sondka Z, Morris NJ, Jackson GH, Cockell SJ, Tainer JA, and Austin CA (2012) MRE11 facilitates the removal of human topoisomerase II complexes from genomic DNA. *Biol Open* **1**:863–873.
- Lee KC, Swan RL, Sondka Z, Padget K, Cowell IG, and Austin CA (2018) Effect of TDP2 on the Level of TOP2-DNA Complexes and SUMOylated TOP2-DNA Complexes. *Int J Mol Sci* **19**:2056.
- Liston DR, and Davis M (2017) Clinically Relevant Concentrations of Anticancer Drugs: A Guide for Nonclinical Studies. *Clin Cancer Res* **23**:3489–3498.
- Lyu YL, Kerrigan JE, Lin C-P, Azarova AM, Tsai Y-C, Ban Y, and Liu LF (2007) Topoisomerase II β mediated DNA double-strand breaks: implications in doxorubicin cardiotoxicity and prevention by dexrazoxane. *Cancer Res* **67**:8839–8846.
- Maede Y, Shimizu H, Fukushima T, Kogame T, Nakamura T, Miki T, Takeda S, Pommier Y, and Murai J (2014) Differential and Common DNA Repair Pathways for Topoisomerase I- and II-Targeted Drugs in a Genetic DT40 Repair Cell Screen Panel. *Mol Cancer Ther* **13**:214–220.
- Malik M, Nitiss KC, Enriquez-Rios V, and Nitiss JL (2006) Roles of nonhomologous end-joining pathways in surviving topoisomerase II-mediated DNA damage. *Mol Cancer Ther* **5**:1405–1414.
- Mao Y, Desai SD, Ting C-Y, Hwang J, and Liu LF (2001) 26 S Proteasome-mediated Degradation of Topoisomerase II Cleavable Complexes. *J Biol Chem* **276**:40652–40658.
- Mårtensson S, Nygren J, Osheroff N, and Hammarsten O (2003) Activation of the DNA-dependent protein kinase by drug-induced and radiation-induced DNA strand breaks. *Radiat Res* **160**:291–301.
- Mirski SEL, Evans CD, Almquist KC, Slovak ML, and Cole SPC (1993) Altered topoisomerase II α in a drug-resistant small cell lung cancer cell line selected in VP-16. *Cancer Res* **53**:4866–4873.
- Misra M, Kuhn M, Löbel M, An H, Statsyuk AV, Sottriffer C, and Schindelin H (2017) Dissecting the Specificity of Adenosyl Sulfamate Inhibitors Targeting the Ubiquitin-Activating Enzyme. *Structure* **25**:1120-1129.e3.

118893

- Moudry P, Lukas C, Macurek L, Hanzlikova H, Hodny Z, Lukas J, and Bartek J (2012) Ubiquitin-activating enzyme UBA1 is required for cellular response to DNA damage. *Cell Cycle* **11**:1573–1582.
- Muslimović A, Nyström S, Gao Y, and Hammarsten O (2009) Numerical analysis of etoposide induced DNA breaks. *PLoS ONE* **4**:e5859.
- Nakamura K, Kogame T, Oshiumi H, Shinohara A, Sumitomo Y, Agama K, Pommier Y, Tsutsui KM, Tsutsui K, Hartsuiker E, Ogi T, Takeda S, and Taniguchi Y (2010) Collaborative action of Brca1 and CtIP in elimination of covalent modifications from double-strand breaks to facilitate subsequent break repair. *PLoS Genet* **6**:e1000828.
- Neale MJ, Pan J, and Keeney S (2005) Endonucleolytic processing of covalent protein-linked DNA double-strand breaks. *Nature* **436**:1053–1057.
- Nitiss JL (2009a) DNA topoisomerase II and its growing repertoire of biological functions. *Nat Rev Cancer* **9**:327–337.
- Nitiss JL (2009b) Targeting DNA topoisomerase II in cancer chemotherapy. *Nat Rev Cancer* **9**:338–350.
- Pommier Y, Sun Y, Huang SN, and Nitiss JL (2016) Roles of eukaryotic topoisomerases in transcription, replication and genomic stability. *Nat Rev Mol Cell Biol* **17**:703–721.
- Riballo E, Kühne M, Rief N, Doherty A, Smith GCM, Recio M-J, Reis C, Dahm K, Fricke A, Krempler A, Parker AR, Jackson SP, Gennery A, Jeggo PA, and Löbrich M (2004) A Pathway of Double-Strand Break Rejoining Dependent upon ATM, Artemis, and Proteins Locating to γ -H2AX Foci. *Mol Cell* **16**:715–724.
- Schellenberg MJ, Appel CD, Adhikari S, Robertson PD, Ramsden DA, and Williams RS (2012) Mechanism of repair of 5'-topoisomerase II–DNA adducts by mammalian tyrosyl-DNA phosphodiesterase 2. *Nat Struct Mol Biol* **19**:1363–1371.
- Schellenberg MJ, Lieberman JA, Herrero-Ruiz A, Butler LR, Williams JG, Muñoz-Cabello AM, Mueller GA, London RE, Cortés-Ledesma F, and Williams RS (2017) ZATT (ZNF451)–mediated resolution of topoisomerase 2 DNA-protein cross-links. *Science* **357**:1412–1416.
- Schellenberg MJ, Perera L, Strom CN, Waters CA, Monian B, Appel CD, Vilas CK, Williams JG, Ramsden DA, and Williams RS (2016) Reversal of DNA damage induced Topoisomerase 2 DNA-protein crosslinks by Tdp2. *Nucleic Acids Res* **44**:3829–3844.
- Smart DJ, Halicka HD, Schmuck G, Traganos F, Darzynkiewicz Z, and Williams GM (2008) Assessment of DNA double-strand breaks and γ H2AX induced by the topoisomerase II poisons etoposide and mitoxantrone. *Mutat Res* **641**:43–47.

118893

- Sunter NJ, Ian G. Cowell, Elaine Willmore, Gary P. Watters, and Austin CA (2010) Role of topoisomerase II β in DNA damage response following IR and etoposide. *J Nucleic Acids* **2010**:710589.
- Tammaro M, Barr P, Ricci B, and Yan H (2013) Replication-Dependent and Transcription-Dependent Mechanisms of DNA Double-Strand Break Induction by the Topoisomerase 2-Targeting Drug Etoposide. *PLoS One* **8**.
- Wang W, Daley JM, Kwon Y, Krasner DS, and Sung P (2017) Plasticity of the Mre11-Rad50-Xrs2-Sae2 nuclease ensemble in the processing of DNA-bound obstacles. *Genes Dev* **31**:2331–2336.
- Willmore E, Frank AJ, Padget K, Tilby MJ, and Austin CA (1998) Etoposide targets topoisomerase II α and II β in leukemic cells: isoform-specific cleavable complexes visualized and quantified in situ by a novel immunofluorescence technique. *Mol Pharmacol* **54**:78–85.
- Xu Q, Farah M, Webster JM, and Wojcikiewicz RJH (2004) Bortezomib rapidly suppresses ubiquitin thiolesterification to ubiquitin-conjugating enzymes and inhibits ubiquitination of histones and type I inositol 1,4,5-trisphosphate receptor. *Mol Cancer Ther* **3**:1263–1269.
- Zeng Z, Cortés-Ledesma F, El Khamisy SF, and Caldecott KW (2011) TDP2/TTRAP is the major 5'-tyrosyl DNA phosphodiesterase activity in vertebrate cells and is critical for cellular resistance to topoisomerase II-induced DNA damage. *J Biol Chem* **286**:403–409.
- Zhang A, Lyu YL, Lin C-P, Zhou N, Azarova AM, Wood LM, and Liu LF (2006) A Protease Pathway for the Repair of Topoisomerase II-DNA Covalent Complexes. *J Biol Chem* **281**:35997–36003.
- Zhao Y, Thomas HD, Batey MA, Cowell IG, Richardson CJ, Griffin RJ, Calvert AH, Newell DR, Smith GCM, and Curtin NJ (2006) Preclinical evaluation of a potent novel DNA-dependent protein kinase inhibitor NU7441. *Cancer Res* **66**:5354–5362.

118893

Footnotes

This study was supported by Bloodwise [Research Specialist Program Grant No. 12031 and Gordon Piller Studentship 13063].

Figure legends

Figure 1. Effect of inhibiting E1 ubiquitin activating enzyme on TOP2-DNA complex levels measured using the TARDIS assay. (A & B) K562 cells were treated for 2 hours with etoposide alone or in combination with 10µM MG132, 10µM MLN7243 or 10µM MG132 and 10µM MLN7243. Cells were incubated for up to a further 2 hours in etoposide-free medium but in the continued presence of DMSO, 10µM MG132 or 10µM MLN7243. Levels of TOP2A- and TOP2B- DNA complexes were measured 0, 0.5, 1 and 2 hours after etoposide removal using the TARDIS assay. Median normalised integrated fluorescence values of three independent experiments are shown (circle symbols) along with the mean \pm SD of the medians. Statistical analyses were performed by two-way ANOVA with comparisons to etoposide alone treatment using Dunett's post-hoc test. **(C)** K562 cells incubated with the indicated concentration of MG132 or MLN7243 for 2 hours. Western blots of whole cell extracts were probed with mab FK2 which recognises all conjugated ubiquitin (mono and poly ubiquitinated proteins).

Figure 2. The appearance of etoposide-induced DSBs is reduced by chemical inhibition of E1 by inhibitor MLN7243 or by siRNA-mediated depletion of E1 ubiquitin activating enzymes. (A) K562 cells were treated with 10µM etoposide (VP-16) alone or in combination with 10µM MG132 for up to 4 hours, and protein-free DSBs were detected by gamma H2AX assay. Median normalized integrated fluorescence for each replica experiment are indicated by small circle symbols, bars represent the means of the median values \pm SD. **(B, C)** The gamma H2AX assay was repeated in K562 cells treated with 10µM VP-16 alone or in combination with 10µM MLN7243 for up to 4 hours. Alternatively, cells were treated for 2 hours with etoposide followed by etoposide washout (WO) and 2 hours incubation in etoposide-free medium with or

118893

without MLN7243 (2+2hr WO). **(D)** gamma H2AX levels were quantified after 2Gy irradiation in the presence and absence of 10 μ M MLN7243, then normalised to a 1-hour post-irradiation control. **(E, F)** gamma H2AX assay following siRNA silencing of UAE1 and UBA6. All values are normalised to a 1-hour 10 μ M etoposide positive control. The medians from independent experiments are shown on each bar. Statistical significance was determined by two-way ANOVA (Bonferroni's post-hoc test).

Figure 3 The effect of siRNA-mediated depletion of UAE1 on the processing of etoposide-induced TOP2-DNA complexes (A) K562 cells were treated with UAE1 siRNA for 72 hours and then incubated for 2 hours with 100 μ M VP-16 or 0.2% DMSO, followed by etoposide removal and a further 2 hours incubation in etoposide-free medium. Cells were collected at 0, 0.5, 1, and 2 hours after etoposide removal and TOP2-DNA complex levels were quantified by TARDIS assay. Statistical comparisons were made by two-way ANOVA with Bonferroni's post-hoc test. **(B)** siRNA knockdown of UAE1 for 24, 48, 72 and 96 hours in K562 cells was tested by western blot probing for UAE1.

Figure 4 MLN7243 inhibits the ubiquitination of TOP2-DNA complexes. (A) K562 cells transfected with control siRNA, UAE1 and UBA6 siRNA or no siRNA were treated with 0.1% DMSO or 10 μ M MG132 for 2 hours. Cells without siRNA were also treated with 10 μ M MLN7243 to compare levels of ubiquitination activity with UAE1/UBA6 knockdown cells. Total ubiquitination levels were examined by western blot, probing with clone FK2 antibody which detects all conjugated ubiquitin. **(B)** K562 cells were treated with 100 μ M etoposide alone or in combination with 10 μ M of the UAE inhibitor MLN7243 for 2 hours and levels of ubiquitinated TOP2-DNA complexes were measured using the TARDIS assay. **(C)** Control cells (CON siRNA) and double UAE1/UBA6 siRNA knockdown cells were treated with 100 μ M etoposide for 2 hours, and levels of ubiquitinated TOP2-DNA complexes quantified using the TARDIS assay (n=3), medians of independent experiments are shown as circles on the bar charts. Statistics was done using two-way ANOVA. Significance comparisons were made by t-test (B) or one-way ANOVA with Tukey's post hoc test (C).

Figure 5. BMI1/RING1A is involved in the processing of TOP2-DNA complexes to protein-free DSBs. (A) K562 cells were treated 100 μ M etoposide (VP-16) alone or

118893

in combination with 90 μ M PRT4165 for 2 hours. Cells were incubated in etoposide-free medium containing DMSO or 90 μ M PRT4165 to maintain inhibition of BMI1/RING1A for 0, 0.5, 1 or 2 hours, and levels of TOP2A- and TOP2B- DNA complexes were measured using the TARDIS assay. Averages were normalised to the 2-hour continuous 100 μ M etoposide control (0 hours after VP-16 removal), and statistical comparisons were made by two-way ANOVA with Bonferroni's post hoc test **(B)** K562 cells were treated with 100 μ M etoposide alone or in combination with 90 μ M PRT4165 for 2 hours. Cells were collected and processed as per the TARDIS assay, and slides were probed with anti-ubiquitin antibody clone FK2. Averages were normalised to a 2-hour 100 μ M etoposide control, and statistical comparisons were made by one-way ANOVA. **(C)** Cells were treated continuously with 100 μ M etoposide alone or in combination with 90 μ M PRT4165 for up to 4 hours, and levels of protein-free DSBs were measured using the γ H2AX assay. Average integrated fluorescence values were normalised to the mean 1-hour 100 μ M etoposide treatment value, and statistical comparisons were made by two-way ANOVA with Bonferroni's post-hoc test. Medians of independent experiments are shown as circles on the bar charts.

Figure 6. Inhibition of ubiquitin activating enzyme or BMI1/RING1A sensitises cells to etoposide. Nalm-6 **(A)** or Nalm-6^{TOP2B-/-} **(B)** cells were incubated with increasing concentrations of etoposide (VP-16) alone or in combination with 400 nM MLN7243 for 120 hours. Growth inhibition was determined by XTT assay. IC₅₀ values (the etoposide concentration resulting in 50% growth inhibition) were determined by plotting dose-response curves, resulting *pf*₅₀ values (the fold difference in IC₅₀ values) are shown on the plots. Data plotted are the mean values from at least three separate experiments \pm SEM. Nalm-6 **(C)** or Nalm-6^{TOP2B-/-} **(D)** cells were incubated with increasing concentrations of etoposide (VP-16) alone or in combination with 35 μ M PRT4165 for 120 hours. Growth inhibition, IC₅₀ and *pf*₅₀ values were determined as for A and B.

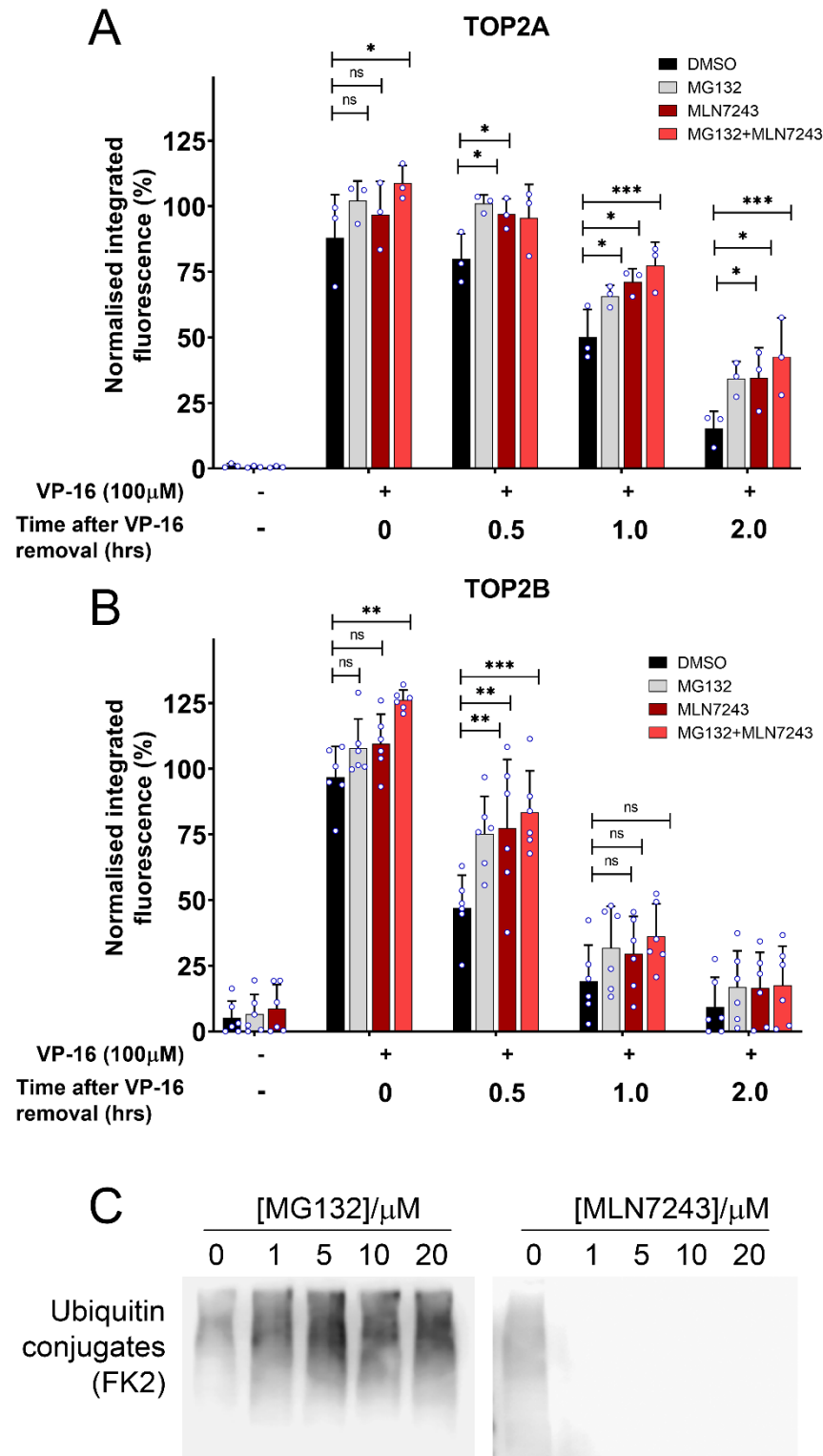


Fig. 1

118893

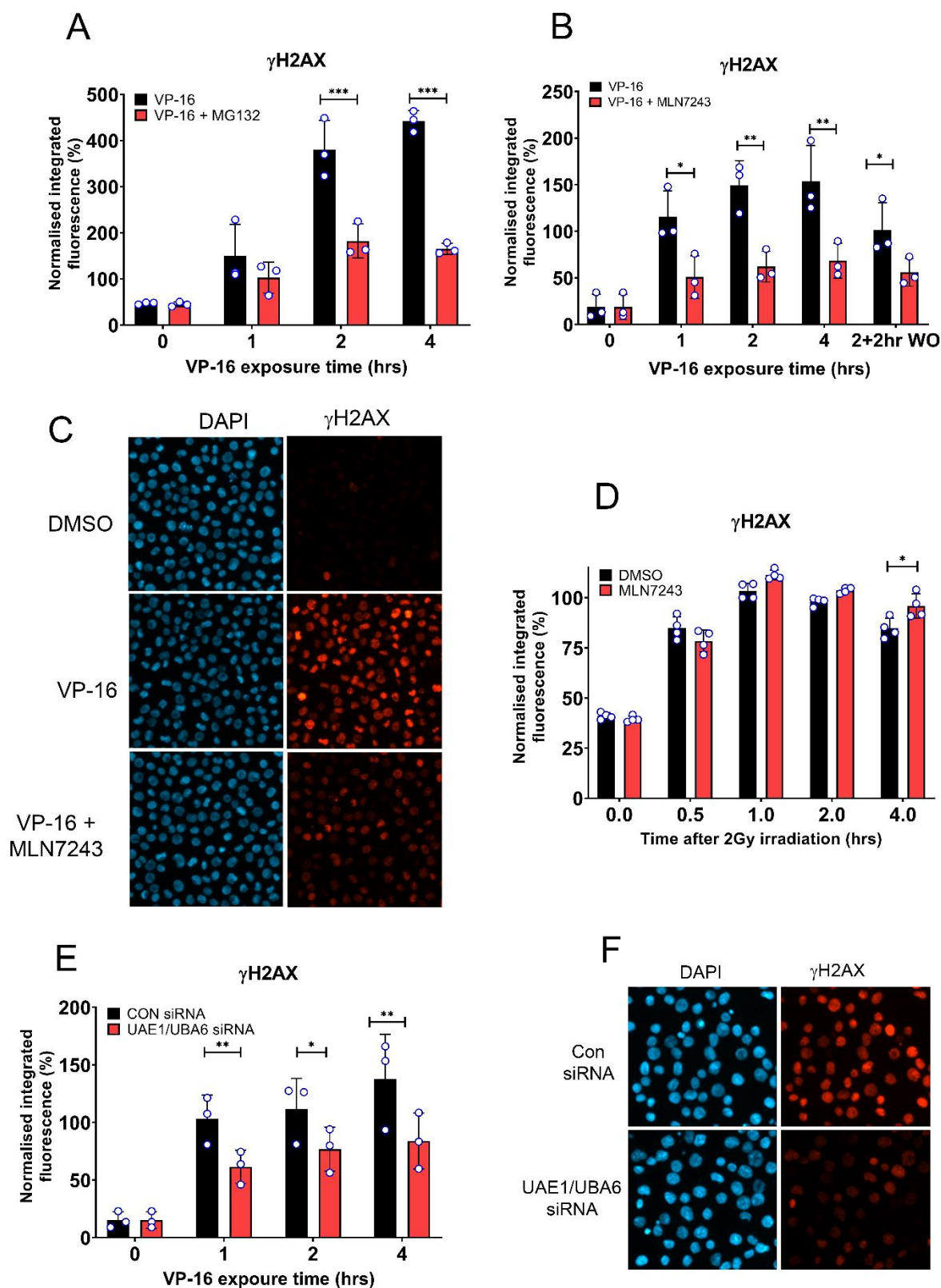


Fig. 2

118893

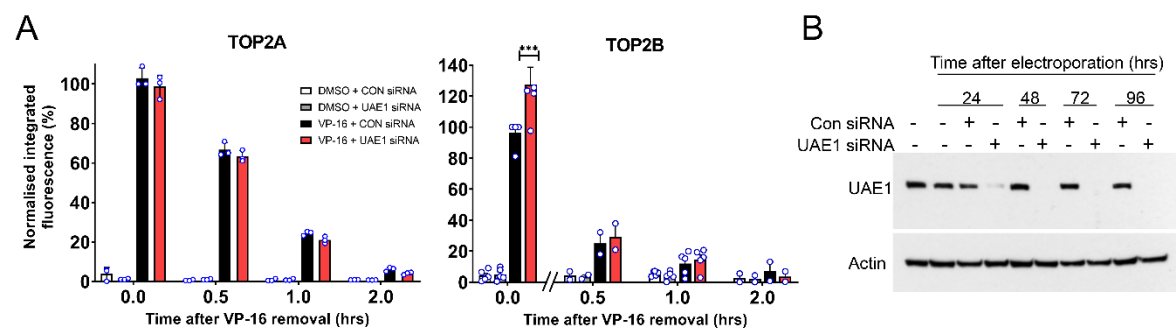


Fig. 3

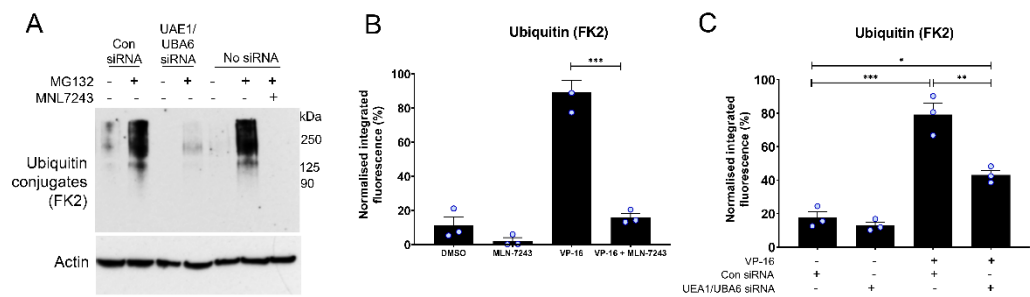


Fig. 4

118893

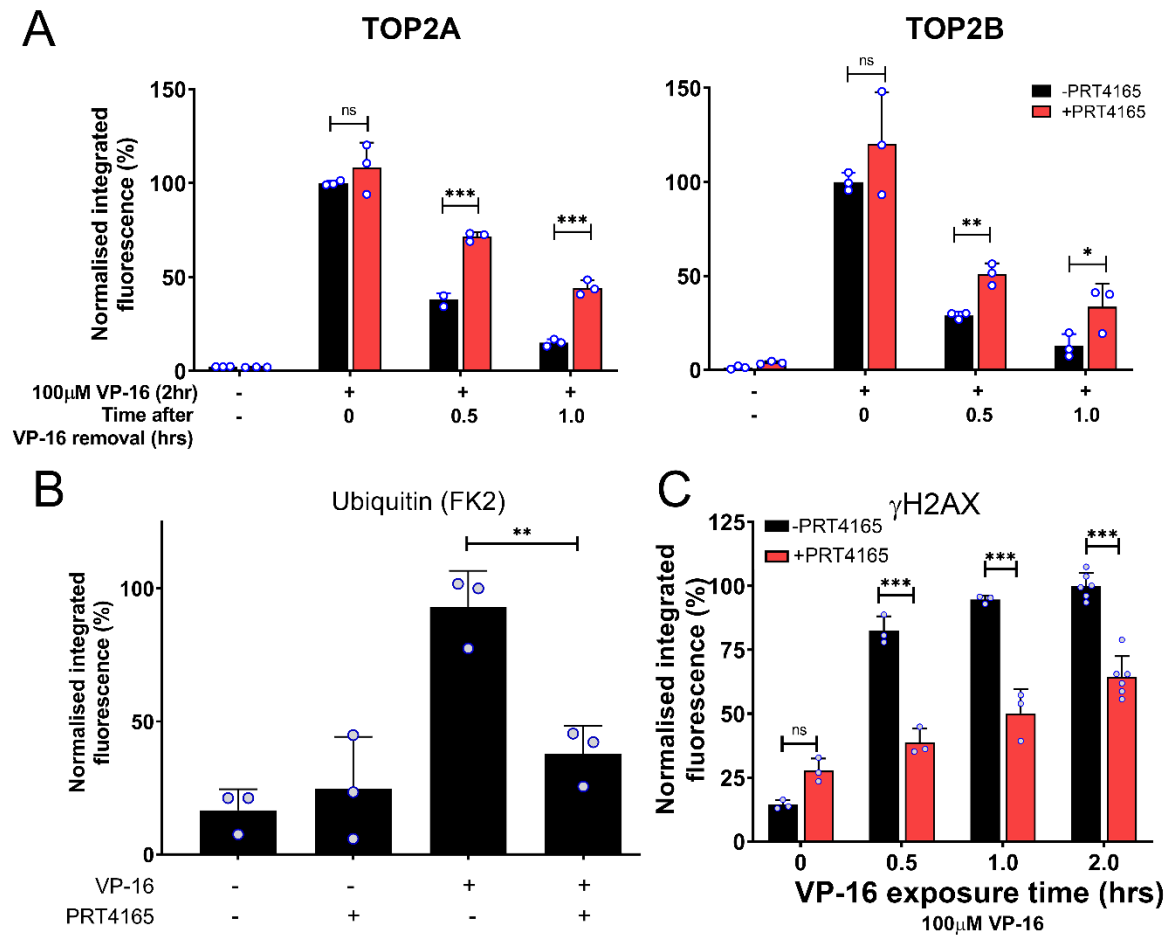


Fig. 5

118893

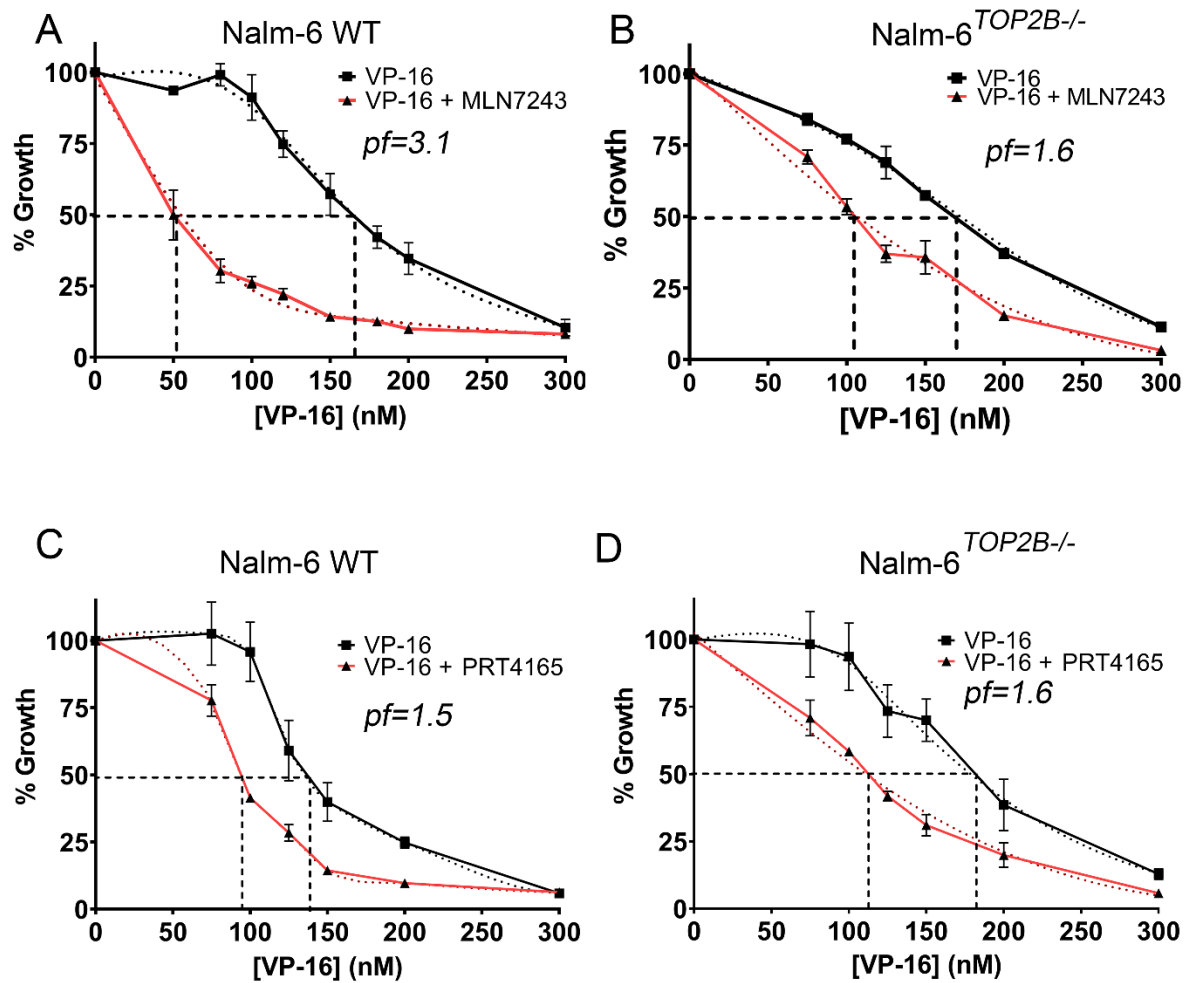


Fig. 6